論文 / 著書情報
Article / Book Information

題目(和文)	高複屈折性材料を指向した棒状液晶分子の合成と相構造および光学特性の評価
Title(English)	Synthesis, phase structures and optical properties of calamitic liquid crystalline molecules for high birefringence materials
著者(和文)	荒川優樹
Author(English)	yuki arakawa
出典(和文)	学位:博士（工学）, 学位授与機関:東京工業大学, 報告番号:甲第9762号, 授与年月日:2015年3月26日, 学位の種別:課程博士, 審査員:小西　玄一,扇澤　敏明,芹澤　武,古屋　秀峰,戸木田　雅利
Citation(English)	Degree:, Conferring organization: Tokyo Institute of Technology, Report number:甲第9762号, Conferred date:2015/3/26, Degree Type:Course doctor, Examiner:,,,,
学位種別(和文)	博士論文
Category(English)	Doctoral Thesis
種別(和文)	要約
Type(English)	Outline

博士論文要約

Synthesis, phase structures and optical properties of calamitic liquid crystalline molecules for high birefringence materials

Yuki Arakawa

2015

Department of Organic and Polymeric materials

Tokyo Institute of Technology

General introduction

1. Applications of calamitic liquid crystalline materials

Since the discovery of the liquid crystal (LC) phase in cholesteryl benzoates and acetates by the Austrian botanist Friedrich Reinitzer in 1888, over 80,000 LC molecules have been synthesized. So far, LC molecules have been applied for the preparation of various optical, electrical, and strength materials by taking advantage of their anisotropic properties, response to external fields, and ability to self-assemble. Representative examples include LC displays such as those used in televisions, personal computers, and mobile phones. In particular, nematic LC materials containing calamitic (or rod-like) molecules are of high importance and have practical applications in LC displays (twisted nematic (TN), super twisted nematic (STN), and polymer-stabilized blue phase LCs).[1]

Over the last two decades, LC materials with high birefringence have been extensively investigated for new applications. Such materials have a small cell gap and small film thickness, which lead to a short response time that is advantageous in the applications discussed above. These materials can also be employed for various optical and electronic applications such as cholesteric films (selective reflection films, wide reflection films, and laser emission films),[2] photostorage devices for holographic applications,[3] and LC lenses.[4] In this thesis, the term "high-birefringence material" is applied to nematic LC materials with positive birefringence, such as calamitic molecules.

A general description of LCs and their optical properties is provided in Section **2**. Subsequently, the nematic phase and optical properties of calamitic molecules are discussed in Section **3**. The context and purpose of this thesis is discussed in chapter Section **4**.

2. Brief overview of LCs

2-1. Liquid crystal

LC phase is located between the three-dimensional crystal phase and the isotropic liquid phase in thermodynamic phase diagrams (Fig. 1) and possess remarkable features hovering between the properties of liquids and crystals. In particular, LCs not only possess various anisotropic properties associated with crystals, but also exhibit liquid fluidity. The LC materials may be divided into two main categories depending on whether they exhibit thermotropic or lyotropic mesophases. The former is observed when the temperature is changed, whereas the latter occurs in suitable solvents and is observed when the solute concentration is changed. In other words, lyotropic LC materials are usually mixtures. Additionally, some LC molecules exhibit both thermotropic and lyotropic mesophases, which are known as amphotropic mesophases.

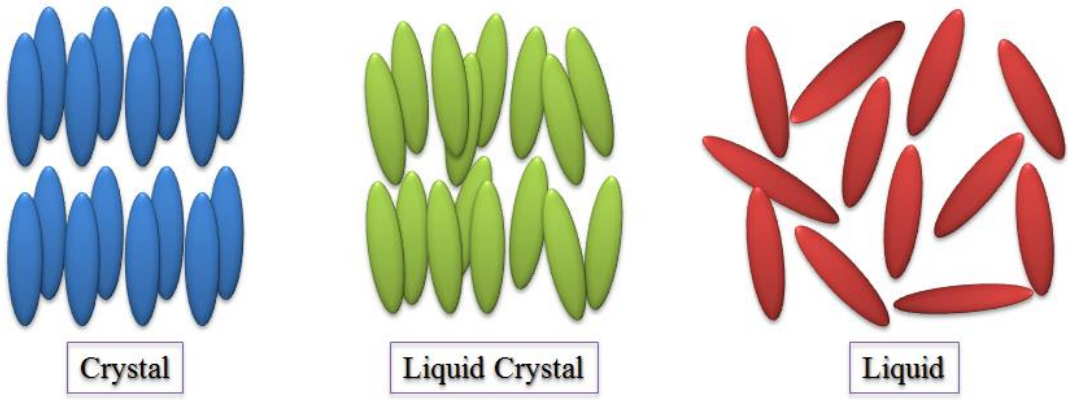

Fig. 1. Schematic descriptions of crystal, LC, and liquid phases.

2-2. Thermotropic LCs

Thermotropic LC molecules are further classified based on their molecular shapes, into calamitic and discotic molecules, and the representative molecular structures are shown in Fig. 2. Generally, calamitic LC molecules are composed of a rigid part (the so-called mesogens)

such as cyclohexyl rings and unsaturated bonding (aromatic rings, alkenes, and alkynes) and a flexible part such as alkyls, alkoxys, and esters, and are fabricated into rod-like shapes. On the other hand, discotic LC molecules are containing a circular core consisting of large π-conjugated molecules such as triphenylene and pyrene, and many flexible tails, which are attached to the discotic core. Generally, both types of LC molecules generate various mesophases, owing to the microphase separations between the mesogenic and flexible parts, induced by the excluded volume effect and van der Waals interactions.

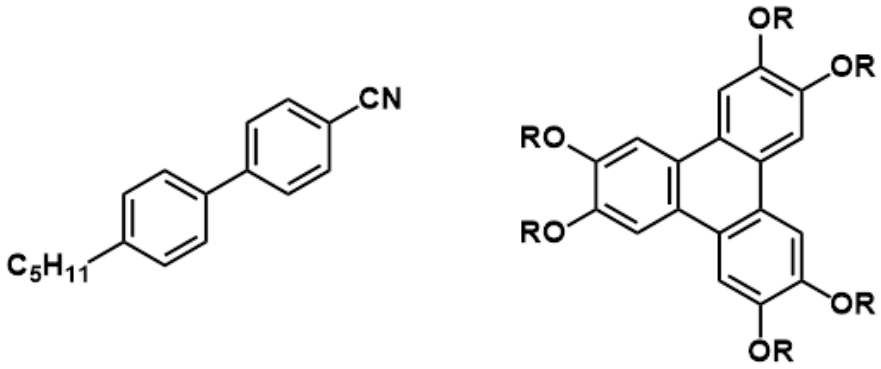

Fig. 2. Representative molecular structures of calamitic and discotic molecules.

2-3. LC phase categories

Thermotropic LC phases are mainly categorized into three types based on the orientational order or translational freedom, namely the nematic phase, smectic phase, and columnar phase. The three LC phases are schematically depicted in Fig. 3.

(1) **Nematic phase** (Fig. 3(a)):The nematic phase contains rod-like molecules as well as discotic molecules, which are termed as the calamitic nematic and discotic nematic phases, respectively. Since the nematic phase has translational freedom in all the three directions, there is no layer structure and it is considered to be the most fluid LC phase.

(2) **Smectic phase** (Fig. 3(b)): Smectic phases have translational freedom in two directions, as a result of which they have a layer structure and the molecules can exhibit liquid behavior in

each layer. In addition, there are various types of smectic phases, depending on whether the molecules are tilted at each layer.

(3) **Columnar phase** (Fig. 3(c)): Columnar phases usually consist of one-dimensional columnar aggregations of discotic or polycatenar molecules, and the columnar aggregations form hexagonal and rectangular lattices. There are various types of columnar phases, depending on molecular tilt in the layers, similar to the smectic phases.

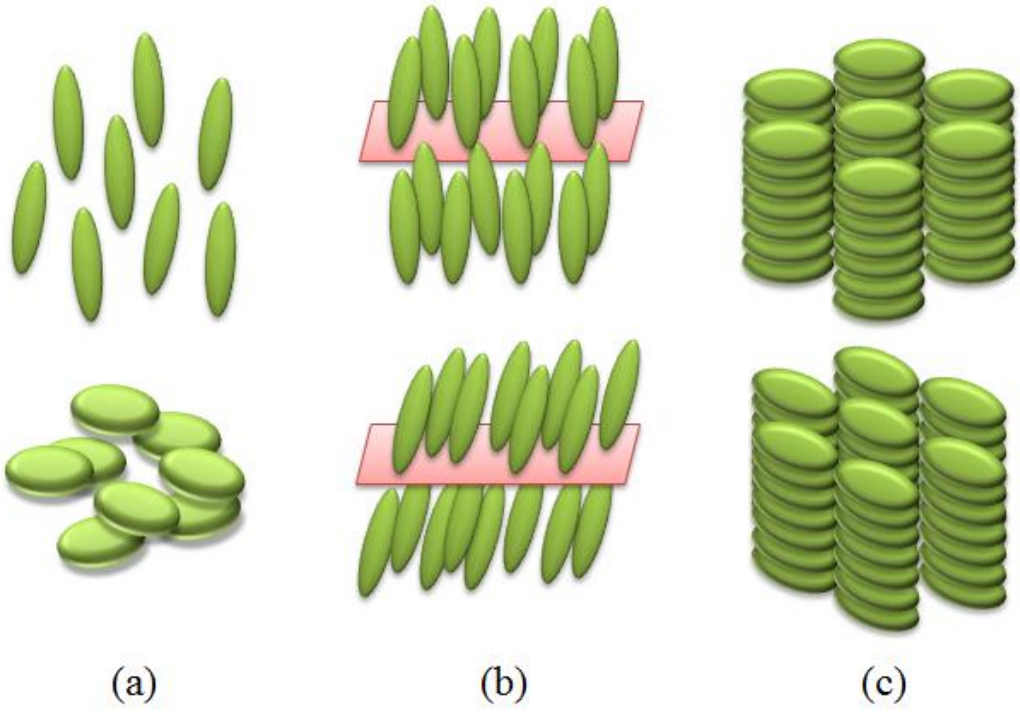

Fig. 3. Schematic images of the (a) nematic phase, (b) smectic phase, and (c) columnar phase.

2-4. LC polymers[1,5]

The LC phases are not only observed in low-molar mass compounds, but also in polymers. A number of LC polymers (LCPs) have been reported to date. The first reported LCP was a lyotropic LC from tobacco mosaic viruses in 1937.[6] In addition, a variety of thermotropic LCPs were developed in the 1960s. LCPs have mesogenic parts in the main chain, side chain, and hybrid chains, which are shown in Fig. 4.

The properties of LCPs include a combination of properties of polymers and low-molar mass LCs. In the case of main-chain LCPs, since their mesogenic parts are directly connected in the main chain, their mobility is highly restricted. As a result, their structures become rigid, resulting in poor processability and response to external fields. However, they have high thermal stability and strength. Therefore, main-chain LCPs are usually used in applications where heat-resistant and high-strength materials (fibers) are required. An example of such a material is Kevlar.

In the case of side-chain LCPs, the mesogenic parts and polymer chains are usually connected via alkyl chains of a certain length (*e.g.*, hexyl chains). In addition, the mobility of the mesogens is not strongly restricted by the polymer chains. Therefore, the properties of side-chain LCPs more closely resemble those of low-molar mass LC compounds than main-chain LCPs. As a result, side-chain LCPs are appropriate for optical applications. The properties of hybrid LCPs are similar to those of side-chain LCPs.

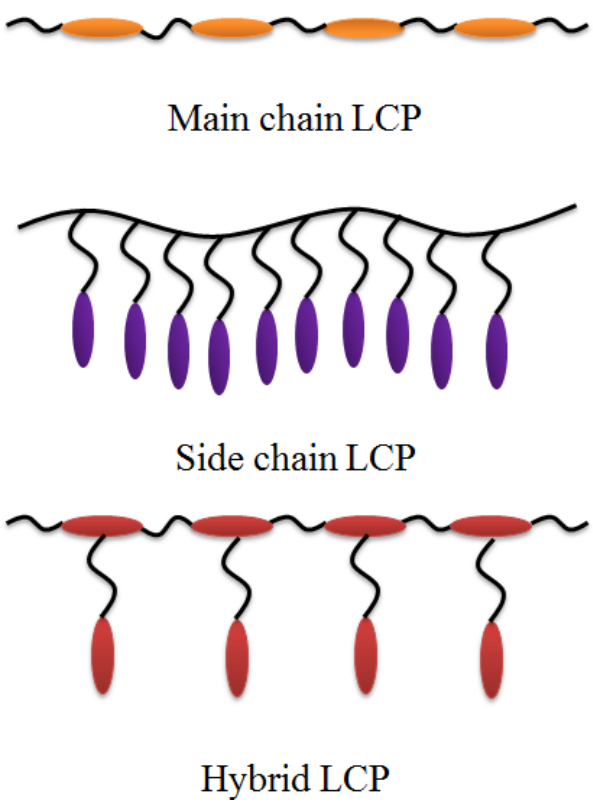

Fig. 4. Schematic descriptions of the structures of LCPs.

2-5. Optical properties of LCs[1,7]

For electro-optical applications, the optical properties of anisotropic LC materials are described by the refractive indices, which are defined by an optical indicatrix having up to three principal refractive index axes, as shown in Fig. 5

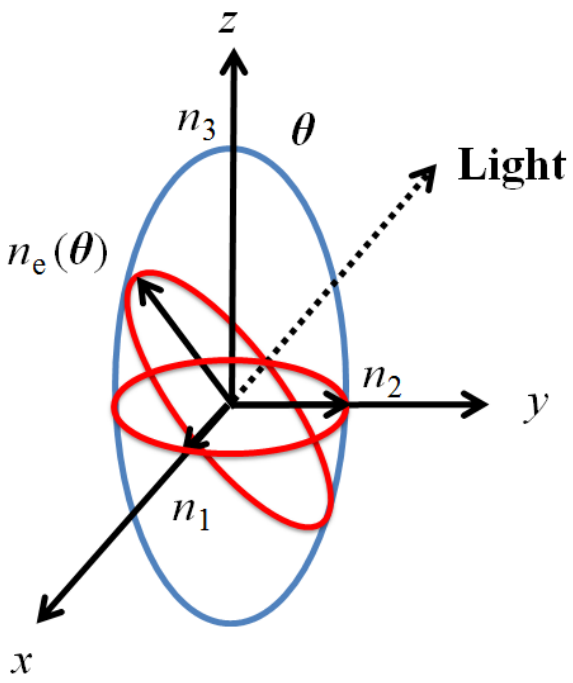

Fig. 5. Optical indicatrix.

$$\frac{x^2}{{n_1}^2} + \frac{y^2}{{n_2}^2} + \frac{z^2}{{n_3}^2} = 1 \qquad (1)$$

In the above equation, n_1, n_2, and n_3 represent the three principal refractive indices, and x, y, and z are the corresponding directions along the three principal axes.

For the uniaxial phases, including the calamitic and discotic nematic phases as well as the orthogonal (non-tilted) smectic and columnar phases, n_1 is equal to n_2, *i.e.*, there are two principal axes. In this case, n_3 is the optical axis, and the indicatrix is symmetric about the n_3

axis. A light beam entering a uniaxial LC material is split into extraordinary and ordinary rays, which are derived from anisotropic structures similar to the crystal phase. The two rays separately leave the LC medium at different times. As a result, two images appear with respect to the object viewed through an anisotropic LC medium (the so-called double refraction). The difference originates from the extraordinary and ordinary refractive indices (n_e and n_o corresponding to n_3 and n_1 and/or n_2, respectively). This difference is described by birefringence (Δn), which represents the difference between the refractive indices (*i.e.*, $\Delta n = n_e - n_o$). The two refractive indices have different properties. Although an ordinary ray propagates along the wave normal and obeys Snell's law, an extraordinary ray is not parallel to the wave normal. Moreover, an extraordinary ray relies on the angle of incident light and the refractive index (n_e) is defined by the following equation (Eq. 2).

$$n_e = \frac{n_{\parallel} n_{\perp}}{\sqrt{{n_{\parallel}}^2 \cos 2\theta + {n_{\perp}}^2 \sin 2\theta}} \qquad (2)$$

where θ is the angle between the n_3 axis and the transmitted light. For $\theta = 0$, *i.e.*, when the incident light enters along the optical axis, $n_e = n_{\perp} = n_o$. In this case, the light can transmit without change in the polarizability, *i.e.*, the material behaves as an optically isotropic medium. Further, there are types of two birefringence properties, namely positive ($n_e > n_o$, $\Delta n > 0$) and negative ($n_e < n_o$, $\Delta n < 0$) birefringence. Positive birefringence typically occurs for general uniaxial calamitic molecules or LC phases, including nematic and smectic A phases, whereas negative birefringence occurs in the cholesteric phase (chiral nematic phase) and discotic LC phase, as schematically described in Fig. 6.

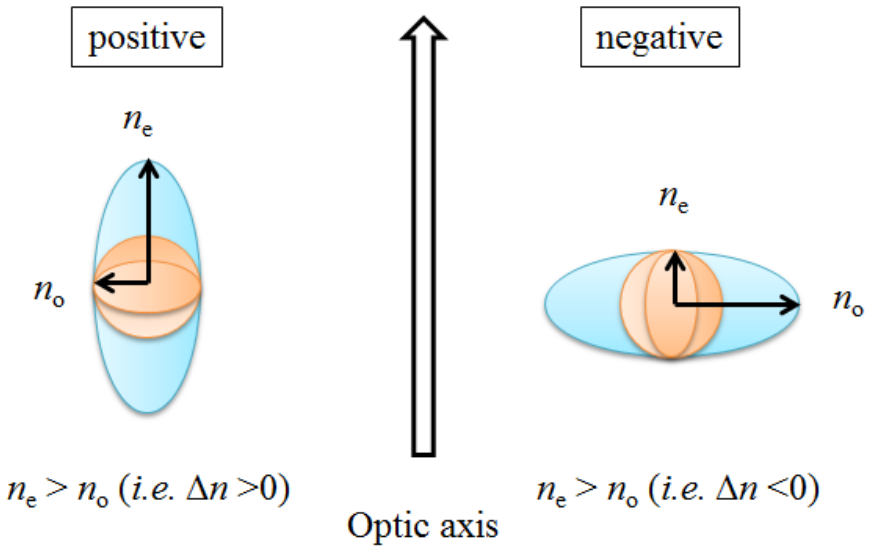

Fig. 6. Schematic descriptions of positive and negative birefringences.

When all the three refractive indices are different, *i.e.*, $n_1 \neq n_2 \neq n_3$, there can be two optical axes perpendicular to the cross section of the optical indicatrix. Such phases are optically biaxial and include the biaxial nematic, tilted smectic, and columnar phases.

3. High-birefringence materials

In order to develop high-birefringence materials, calamitic molecules exhibiting the nematic phase are very important, since they exhibit large positive birefringence, and can be easily aligned by applying an external force, owing to their fluidity. In this Section, the structure and optical properties of the nematic phase and their molecular design are described.

3-1. Nematic phase[1,7]

Generally, the nematic phase is usually described as a one-dimensional ordered elastic liquid, which has no long-range positional order or layers. The average direction, called the nematic director (**n**) is the orientational order of the molecular long axis, as schematically depicted in

Fig. 7. Molecules along the director as well as those pointing in the opposite direction (rotated by 180°) are regarded as equivalent. Therefore, the molecules have a disarrayed head to tail arrangement, where **n** = **-n**. Thus, this phase has rotational symmetry with respect to the director. The degree of orientational order in the direction along the director is given by the order parameter (**S**). Typically, the following equation (Eq. 3) is used to describe the nematic phase.

$$S_2 = \frac{1}{2} < 3cos^2\theta - 1 > \qquad (3)$$

where θ represents the angle between the individual molecules and the director, and the brackets in the equation indicate the temporal-spatial average for the assembly of molecules. In the above equation, S_2 is the scholar order parameter, which is equal to the average of the second Legendre polynomial ($S_2 = <P_2>$), which describes the phase transition from the isotropic to the nematic phase. S_2 values of 0 and 1 indicate random molecular order (*i.e.*, isotropic liquid) and perfectly oriented molecules along the director, respectively. For a typical nematic phase, experimental values of the scholar order parameter are between 0.3 and 0.7. When the isotropic phase transitions to the nematic phase, the value is relatively small, and it increases with decreasing temperature.

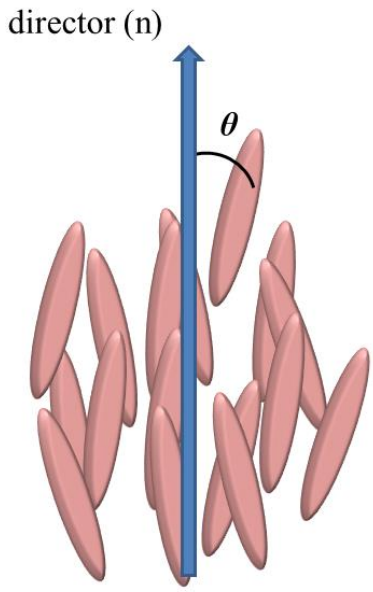

Fig. 7. Nematic phase.

3-2. Optical properties of the nematic phase[1,7]

Based on the optical properties, the nematic phase may be broadly classified into three types, namely the uniaxial nematic phase with positive birefringence, uniaxial nematic phase with negative birefringence, and the biaxial nematic phase. The uniaxial nematic phase is of most interest, since typical high-birefringence materials exhibit this phase.

As mentioned above, calamitic molecules of the nematic phase exhibit positive birefringence ($n_e > n_o$ and $\Delta n > 0$). In this case, the molecular long axis and short axis correspond to n_e and n_o, respectively, which have slightly different dependence on temperature. Generally, n_e decreases with increasing temperature, whereas n_o slightly increases with increasing temperature. Consequently, Δn decreased with an increase in the temperature. Therefore, experimentally observed behavior can be understood based on the equation relating the anisotropic refractive indices with the molecular polarizability anisotropies. In general, for the refractive index of an isotropic medium, the Lorentz-Lorentz equation (given by Eq. 4), which relates the microscopic molecular polarizability with the macroscopic refractive index, is as follows:

$$\frac{(n^2 - 1)}{(n^2 + 2)} = \frac{\rho N_A \alpha}{3M\varepsilon_0} \qquad (4)$$

In the above equation, n is the mean refractive index, ρ is the molecular density, α is the molecular polarizability, M is the molecular weight, N_A is the Avogadro's number, and ε_0 is the permittivity of vacuum. Eq. 4 is often applied to anisotropic fluid media (nematic LCs).[8]

$$\frac{({n_e}^2 - 1)}{(n^2 + 2)} = \frac{\rho N_A \alpha_e}{3M\varepsilon_0} \qquad (5(a))$$

$$\frac{({n_o}^2 - 1)}{(n^2 + 2)} = \frac{\rho N_A \alpha_o}{3M\varepsilon_0} \qquad (5(b))$$

In the above equations, α_e and α_o are the average polarizability along the directions parallel and perpendicular to the optical axis, respectively. The two parameters, α_e and α_o can be described as a function of the anisotropy of molecular polarizability Δα, which represents the difference between the molecular longitudinal $\alpha_\parallel$ and transverse $\alpha_\perp$ polarizabilities and the orientational order parameter S (Eq. 6(a) and 6(b)).[9]

$$\alpha_e = \alpha + \frac{2}{3}\Delta\alpha S \qquad (6(a))$$

$$\alpha_o = \alpha - \frac{1}{3}\Delta\alpha S \qquad (6(b))$$

In the above equations, α is the mean molecular polarizability ($\alpha = (\alpha_\parallel + 2\alpha_\perp)/3$). Combining equations 5 and 6, the following equation can be derived (Eq. 7).

$$\frac{(n_e{}^2 - n_o{}^2)}{(n^2 + 2)} = \frac{\rho N_A \Delta\alpha S}{3M\varepsilon_0} \qquad (7)$$

Eq. 7 indicates that the birefringence is a function ρ, $\Delta\alpha$, and S. Moreover, since $\alpha_{\parallel}$ is larger than $\alpha_{\perp}$ for calamitic nematic molecules (*i.e.*, $\Delta\alpha = \alpha_{\parallel}-\alpha_{\perp} > 0$), n_e must be larger than n_o, indicating positive birefringence.

From Eq. 5 and 6, it may be seen that the n_e and n_o values are primarily influenced by α_e and α_o, as a result of the temperature dependence of S. With an increase in the temperature, the values of α_e and ρ decrease owing to the decrease in the value of S. Therefore, n_e significantly decreases with an increase in the temperature. On the other hand, the temperature dependence of n_o may be slightly complicated, because α_e and ρ exhibit inverse temperature dependences. For nematic materials with a relatively large value of $\Delta\alpha$, α_o significantly increases with increasing temperature, resulting in an increase in n_o as a function of temperature. For nematic materials with smaller $\Delta\alpha$ values, there is a smaller change in α_o with respect to temperature. When the influence to n_o, which is caused by thechange in ρ and α_o, is the same, the n_o curve is almost flat.

For calamitic nematic materials, n_e, n_o, and Δn also show wavelength dispersion. Generally, these values decrease with increasing wavelength (so-called positive dispersion) and obey Cauchy's equations as described by Wu and coworkers.[10]

3-3. Molecular design of high-birefringence materials

According to Eq. 7, the values of n_e, n_o, and Δn are primarily determined by $\Delta\alpha$ as well as the molar volume ($V = M/\rho$) at a constant reduced temperature, since S depends on temperature.

The Δα value is determined by the molecular structure. On the other hand, for an absorption medium, the refractive indices can be expressed using Eq. 8.

$$n = n_r - jk \qquad (8)$$

where n_r determines the velocity of light in the medium, $j = \sqrt{-1}$, and k represents the absorption coefficient. Therefore, the refractive index is strongly influenced by the electric absorption of molecules.

In general, large conjugated rod-like structures are highly suitable for the preparation of high-birefringence materials, owing to high α_e values and electronic absorption. Therefore, aromatic rings are more effective compared to aliphatic rings such as the cyclohexyl ring, which is also employed as mesogenic cores. The most widely used aromatic ring is the benzene ring, which is fabricated along with linear structures, *i.e.*, para-phenylenes. The most popular high-birefringence materials were cyano biphenyl derivatives represented by 5CB, reported by Gray, Harrison, and Nash in 1973.[11] These materials have attractive characteristics, including high Δ*n* values close to 0.2 and a room-temperature nematic phase. In addition, *ter*-phenyl derivatives, which also exhibit high birefringence, have also been extensively studied.[12] Besides these, various nematic molecules with naphthalene rings have been reported.[13] While these derivatives have extremely high birefringence (Δ*n* > 0.5), their transition temperatures are also relatively high. Finally, heterocyclic molecules have also been employed.[13(a),14]

In order to expand the anisotropic structures, various linkage groups are employed to bridge the ring structures. So far, various molecules containing ester and thioester linkageshave been reported.[15] In particular, high-polarizability groups (bondings) such as

unsaturated linkage groups including alkene, acetylene, di-acetylene, and endiyne, are highly effective for enhancing birefringence. Incorporation of these groups results in high Δα values and/or electric absorption shifts to the long wavelength range.[13,14] For example, nematic LC diphenyl-acetylene derivatives (the so-called tolane-type LC materials) have been used in super twisted nematic (STN) displays.[5,16] Various diaryl-diacetylene derivatives have also been reported.[5,16(b),17] Moreover, the introduction of high-polarizability groups such as halogens, cyano, and isothiocyanate groups at the terminal position of the mesogenic parts, leading to high anisotropy of molecular polarizability, is also very effective. This has been employed in many studies reported in the literature.[5,12-16]

In addition, flexible alkyl spacers at terminal positions and substituents at lateral position are also important, in order to adjust the phase structures and/or the phase transition temperatures.In the case of the former, generally when longer alkyl chains are employed, the transition temperatures can be decreased and some smectic phases are likely to be formed. The latter case is most suitable for decreasing the transition temperature.[18] Usually, relatively small substituents such as fluoride chloride, methyl, and ethyl groups are selected, because larger substituents can strongly affect the refractive index properties.

Calamitic nematic molecules usually exhibit n_e values in the range of 1.4 to 1.9, with Δn values between 0.02 and 0.4. For particularly high-birefringence materials (*e.g.*, $\Delta n > 0.3$), the birefringence tends to be measured from eutectic mixtures, with room temperature nematic materials.[1] Molecular design for high-birefringence materials are shown in Fig. 8.

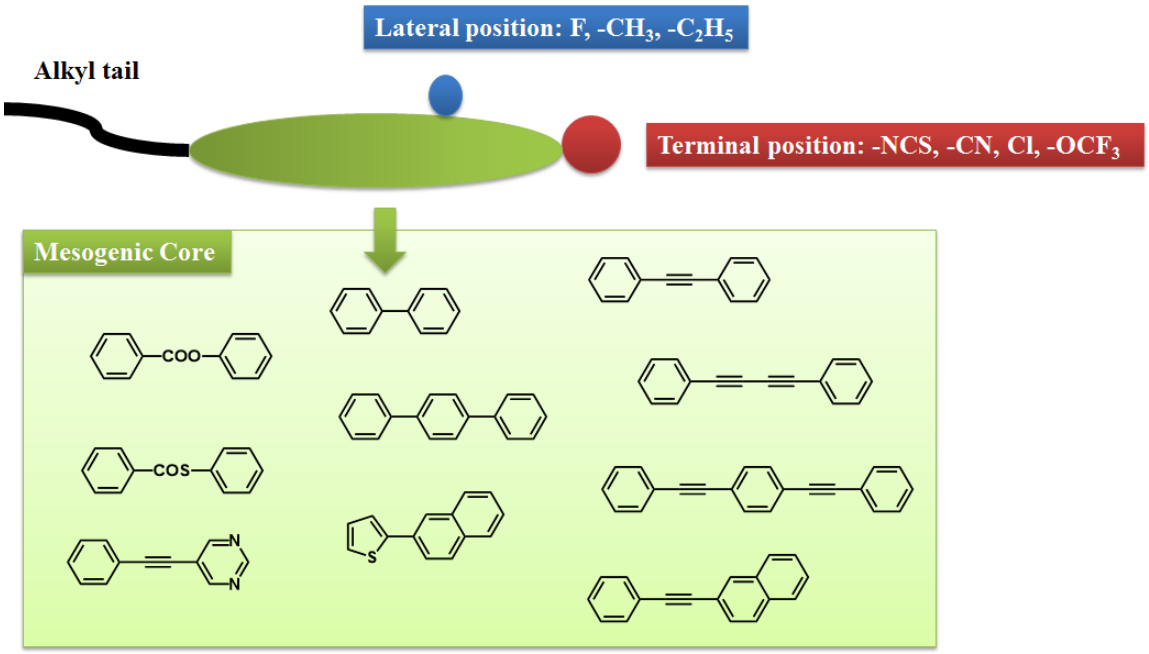

Fig. 8. Molecular design of typical high-birefringence materials.

4. Context and purpose of this thesis

4-1. In-depth investigation of the refractive index and birefringence from single-component systems

In most cases, refractive indices of LC molecules are measured by the Abbe's method, which is widely known as a relatively easy and highly accurate method. The method is based on the measurement of the critical angle between the LC medium and a standard prism whose refractive index is known. Owing to the critical angle measurement principle, the refractive index of the prism is required to be higher than that of the LC medium. However, the choice of the prism is often restricted in the case of high-birefringence LC molecules (or high-refractive index materials), since the high extraordinary ray refractive indices often exceed those of the prisms. In such cases, the critical angle cannot be measured and the refractive indices cannot be calculated. In addition, this method is also restricted by the high transition temperature of LC materials. In a typical Abbe's refractometer, the measurable

temperature is up to 50 °C. Therefore, the refractive indices of LC materials are extrapolated from those of binary or multi eutectic mixtures of room-temperature LC materials. This is a good approach for estimating the refractive indices of LC materials, since it allows easy comparisons with other LC molecules under standard conditions. However, this approach does not take into account the temperature dependence of high-birefringence materials. Determination of refractive indices from a single-component system is important for not only developing and improving materials, but also to obtain a fundamental understanding of the basic chemistry.

In this thesis, I have tried to investigate in detail the refractive indices and birefringences of a single-component system containing target LC materials. They were determined by the interference method, which is based on the interference of extraordinary and ordinary rays for monodomain homogenously aligned nematic LC materials, achieved in a uniaxial rubbing cell. The method is described in detail in Chapters 1-1 and 2-2. Further, the temperature and structure dependence of refractive indices were investigated in detail.

4-2. LC phase structure analysis of conjugated calamitic materials

In most studies, the usual calamitic nematic phases are typically ignored for structure analysis, because they are considered to be highly fluid and as having less complicated structures than other mesophases. High-birefringence calamitic molecules are also included among these materials. Therefore, although high-birefringence nematic materials have been reported, their microscopic structures in the nematic phase are usually not investigated in most studies. However, I believe that investigating these structures is highly important for the development of optical materials, since the refractive indices originate from the aggregation systems as distinct from a single molecule.

Moreover, this topic is very intriguing from the point of view of fundamental scientific understanding. Generally, it is thought that all types of molecules aggregate with each other, forming transitional clusters containing a few molecules in the isotropic phase. In the case of LC phases, these clusters are known as cybotactic clusters. In the cases where larger cybotactic clusters are formed in the nematic phase, they are called "cybotactic nematic phase", which is a term first proposed by De Vries in 1970.[19] This phase has been classified into two main types, namely cybotactic nematic A (N_{cybA}) and C (N_{cybc}).[20] In the former phase, the molecules in the clusters are oriented along the director, *i.e.*, the clusters are similar to the smectic A phase. In the latter case, the molecules in the clusters are tilted with respect to the director, *i.e.*, the clusters are similar to the smectic C phase. These phases are thought to be the origin of the "biaxial nematic phase," which is a controversial type of nematic phase. In recent years, a number of bent-type nematic molecules have been synthesized, since they are known to have relatively large cybotactic clusters, owing to the shape effects.[21] While, there have also been several studies on calamitic nematic molecules for elucidating the cybotactic nematic phase.[19,20(b),22]

In this context, I investigated the phase structures of conjugated calamitic nematic molecules using polarized optical microscope (POM) observations and X-ray diffraction (XRD) measurements, in order to understand the correlations among molecular structures, aggregation states, and refractive indices, as well as to study their features.

4-3. Development of high-birefringence LCPs

As described in Section 2-4, side-chain LCPs are more suitable for preparing high-birefringence materials compared to main-chain LCPs. Since high-birefringence materials consist of multiple aromatic rings, unsaturated bonds, and high-polarizability substitutions, they are likely to lead to highly ordered smectic phases, a property that is

especially pronounced in polymers, since monomers only have nematic phases. Therefore, there have been very few reports on high-birefringence nematic LCPs or even side-chain LCPs so far (Fig. 9). For example, Okano *et al.* have reported a high birefringence value of 0.72 at 633 nm for a side-chain LCP with an azotolane core that exhibits only a nematic phase.[23] In addition, the derivatives of this LCP were also investigated.[24] Furthermore, Kawatsuki *et al.* have reported tolane and bistolane-based side-chain LCPs.[25] Since the above polymers are utilized for common holographic applications, they usually have photoisomerization or photoreactive units. In 2010, Chen *et al.* reported mesogen jacketed-type LCPs, whose mesogenic units are attached laterally to the main chain with or without short spacers, for applications in optical retardation films.[26] These polymers contained conjugated heterocyclic calamitic molecules in the side chain and exhibited high birefringence, as evaluated in their amorphous states. Moreover, there have been several reports on the effect of polymerization on birefringence. Lub *et al.* have reported that the birefringences of polymers that undergo a photocrosslinking reaction between two functionalized monomers are improved compared to the corresponding values for the monomers, owing to increased order parameters.[27] These mesogens are usually not conjugated molecules.

In terms of the refractive indices and/or assembly states, to the best of my knowledge, the relationships between uniaxially aligned nematic polymers having calamitic conjugated mesogens in the side chain and the monomers have never been understood. Therefore, I investigated novel high-birefringence nematic side-chain LCPs, in which calamitic conjugated mesogens were introduced in the side chains. Phase structural analyses and refractive index measurements were conducted for these materials and compared with the values for the monomers. Further, I attempted to prepare a uniaxially aligned high-birefringence polymer

film using a photocrosslinking reaction, by employing conjugated calamitic molecules as monomers.

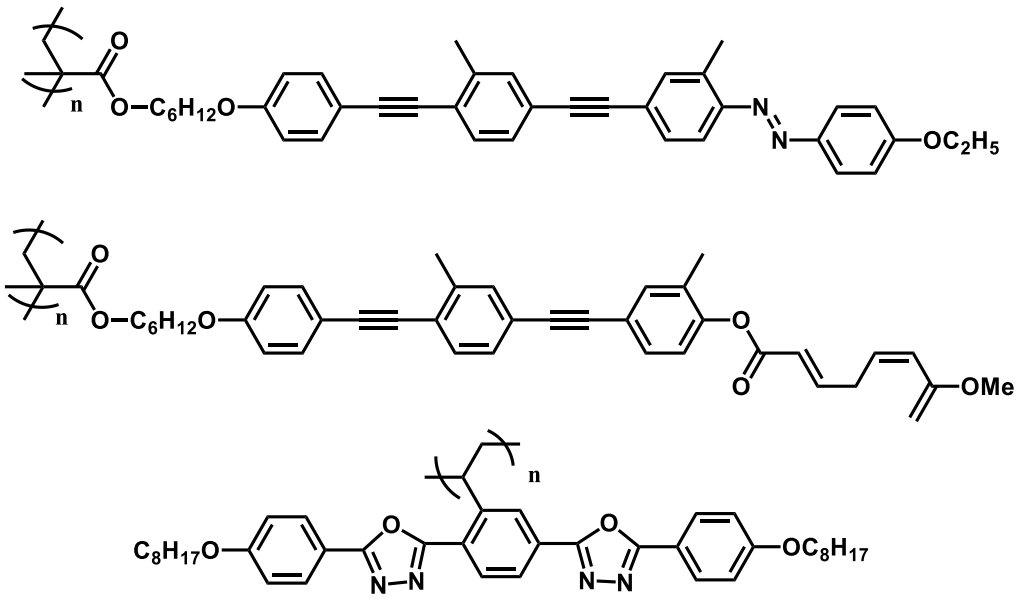

Fig. 9. Molecular structures of various high-birefringence LC polymers.

4-4. Development of novel high-birefringence materials

Sulfur atoms are known to be highly effective in improving the refractive index since they have higher polarizability compared to ubiquitous atoms such as carbon, nitrogen, and oxygen. Therefore, sulfur atoms are also expected to have a beneficial effect on high-birefringence materials.

There have been a few reports on sulfur-containing calamitic nematic materials, whose molecular image is shown in Fig. 10.[28] Seed *et al.* reported that although calamitic molecules having butylsulfanyl groups (SC_4H_9) are good candidates for high-birefringence materials, such molecules have unstable monotropic mesophases, highly ordered smectic phases, or no mesophases.[15(a),29] These are thought to be due to the high level of molecular attractionbetween sulfur-containing molecules because these molecules not only experience high dipole interactions due to high polarizability, but also experience chalcogen interactions

(the so-called S–S contacts), which are attractive interactions derived from intra- or intermolecular n–σ* interactions of sulfur atoms attached to the chalcogen element. In particular, the chalcogen interactions are of great importance in organic electronics[30] and structural chemistry,[31] since they lead to well-organized and/or specific molecular assemblies. Disc[32] and bent-type[33] LC compounds with alkylsulfanyl groups in smectic or columnar phases have been reported.

While thiophene-based rings are categorized into rigid aromatic rings, they are considered to be good candidates for the preparation of LC mesogens. Since they also exhibit similar strong interactions, they have been mainly studied for applications in organic electronics.[34] Therefore, a large number of studies on thiophene-based LC materials with highly ordered smectic phases have been published. Generally, the 2 and 5 positions on the thiophene ring are exclusively substituted; as a result, the ring is slightly bent or has an expanded molecular rotational volume. Moreover, the structure itself makes it difficult for calamitic molecules to generate the nematic phase.[35] So far, various thiophene-based calamitic molecules have been studied.[13(a),14,36] Nevertheless, very few reports exist on the stable nematic phase and refractive index properties.

In the context, I have tried to develop sulfur-containing calamitic nematic molecules including molecules with alkylsulfanyl groups and thiophene-based calamitic molecules as novel high-birefringence nematic materials.

Fig. 10. Molecular image of sulfur-containing rod-like materials.

Abstract

Chapter 1

The results of the refractive index and phase structure analyses of diphenyl-oligoyne molecules, which are comprised of two aromatic rings connected by a single or multiple acetylene bonds, are described in **Chapter 1** (Fig. 11). In LC chemistry, examples of such molecules include the diphenyl-acetylene derivatives (the so-called tolane-type molecules).[16] As mentioned previously, these molecules have been used for LC displays. Moreover, diphenyl-diacetylene (DPDA) molecules are also known to be nematic molecules that exhibit high birefringence values. LC DPDA derivatives were first reported by Grant in 1978.[17(a)] Subsequently, Wu *et al.* reported their high birefringence properties in 1989.[17(b)] Since then, a number of DPDA derivatives have been synthesized for various LC applications.[17] These molecules not only exhibit higher birefringences (or refractive indices), but also have more stable nematic phases compared to those of tolane-type LC materials. These properties may allow us to investigate the dependence of refractive indices and phase structures on the temperature and homologous series length, for both alkyl chains and ring structures. Owing to the reasons mentioned in Section 4-1, these materials have mostly been evaluated in eutectic mixtures. Moreover, their microphase structures in the mesophases have also not been understood yet.

In **Chapter 1-1**, I describe the synthesis of two series of DPDA materials, containing alkyl and alkoxy tails with lengths of *m* at both of the terminal positions (DPDA-C*m* and DPDA-OC*m*, respectively). The dependence of the birefringence properties of these materials on temperature, substitution, and chain length are described in detail. In **Chapter 1-2,** the investigation is extended to diphenyl-acetylene (tolane LC materials) and diphenyl-triacetylene (DPTA) materials, in order to understand the effect of acetylene bonds on the refractive indices and LC phases of diphenyl-oligoyne LC molecules with the same

alkoxy tails and an m value of 6. In **Chapter 1-3**, I describe the synthesis of fluorinated DPDA-OC*m*, where fluorine was substituted at the ortho-positions, next to the terminal alkoxy tails, in order to decrease the phase transition temperatures for obtaining more useful materials. The effect of fluorine on the refractive indices and thermal transition behaviors were evaluated in detail. In **Chapter 1-4**, investigations on the nematic phases of DPDA-OC*m* and the fluorinated DPDA-OC*m* using POM observations and XRD measurements are described in detail. In addition, these phases were compared to determine the effect of fluorine on the LC phase structures. In **Chapter 1-5**, the synthesis of polymethacrylate with a DPDA moiety in the side chain is described, in order to develop high-birefringence side chain LCPs.

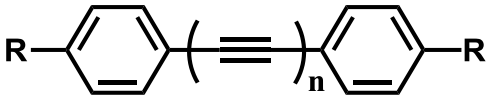

Fig. 11. Molecular structure of diphenyl-oligoynes.

Chapter 2

The refractive indices and birefringence properties of dinaphthyl-oligoynes, wherein the phenyl rings of diphenyl-oligoynes are replaced with naphthyl rings at the 2, 2′-positions (Fig. 12), are outlined in **Chapter 2**. Since naphthalene has a more anisotropic structure and higher polarizability than benzene, it is often incorporated into calamitic nematic materials for obtaining high-birefringence materials.[13] Furthermore, incorporating naphthalene is effective for achieving the nematic phase. Linearly conjugated structures can be fabricated by substitution at the 2,6-position. However, these structures are less anisotropic than linear para-phenylenes. For example, Uchimura *et al.* reported that bisbiphenyl-diacetylene

derivatives exhibited not only high transition temperatures, but also highly ordered smectic I and J phases, and therefore their birefringences could not be measured.[38] Meanwhile, Hsu *et al*. reported that dinaphthyl-diacetylenes showed exclusively enantiotropic nematic phases.[39] However, their refractive indices and birefringence properties are unknown, although these materials are expected for new extremely high-birefringence nematic materials.

Dinaphthyl-acetylenes, which can be classified under tolane homologs, are also expected to be high-birefringence nematic materials, and are more useful for practical applications. However, although they have simple structures, there are no detailed reports regarding them in the literature.

In order to realize extremely high birefringence properties, in **Chapter 2-1**, I describe the design of dinaphthyl-diacetylenes with alkoxy tails at both the terminal positions (DNDA-OC*m*). The dependence of their transition behaviors and birefringence properties on the temperature and number of carbon atoms have been investigated in detail. In **Chapter 2-2**, I describe the accurate determination of n_e and n_o of highly birefringent DNDA-OC*m* by the multiple-beam interference method and their dependence on temperature and alkyl carbon number. In **Chapter 2-3**, I describe the synthesis of dinaphthyl-acetylenes with alkoxy tails having a length of m (DNA–OC*m*), as novel high-birefringence materials. The transition behaviors and birefringence properties of their homologs containing different alkoxy tails lengths, were investigated in detail. In **Chapter 2-4,** the design of side chain LCPs, *i.e.*, polymethacrylates having DNA mesogens in the side chain, are described, in order to develop new high-birefringence nematic LCPs.

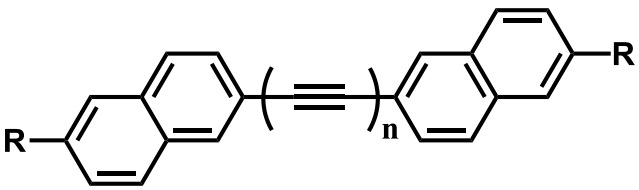

Fig. 12. Molecular structure of dinaphthyl-oligoynes.

Chapter 3

A summary of the phase structures, refractive indices, and birefringences of bistolane-based materials is provided in **Chapter 3**. Bistolanes, which were reported first by Pugh and Percec in 1990, consist of three benzene rings connected by two triple bonds joined at the p,p′-positions of the central benzene (Fig. 13).[40] Since they form linear π-electron conjugated structures, they are more favorable for use as high-birefringence LCs than other molecular core units such as tolane, DPDA, and biphenyl. Consequently, bistolane-based materials have received attention.[41] Moreover, since not only both of the terminal positions, but also various lateral positions of bistolane can be substituted owing to the presence of thecentral ring, its structure is appropriate for various functionalizations. There have been several reports in the literature regarding the introduction of alkyl, alkoxy, cyano, and thiocyanate groups at terminal positions as well as methyl and ethyl groups at the lateral positions. In particular, in the latter case, it is known that the transition temperatures of the bistolane materials are decreased and their nematic phases are expanded. These features are very important, not only from the view point of their use in various applications, but also in terms of basic scientific understanding. However, the birefringence properties and phase structures of single component systems of bistolanes are yet to be reported. This is also true for fluorinated derivatives, where the effects of fluorine and its position have not been investigated yet.

Bistolane-based molecules have more thermal and photo stability than diacetylenes. Therefore, if a molecular design of bistolanes exhibiting relatively low transition temperatures and a wide nematic phase range can be achieved, they can be employed for photo-crosslinking polymerizations, that are required for high-birefringence uniaxial films.

In **Chapter 3-1**, the design and synthesis of three types of bistolane-based LC molecules are described, two of which have fluorine atoms at other positions, in order to elucidate the fluorine substitution effects between the assembly states and the optical properties of LC

materials. In **Chapter 3-2**, I describe the preparation of mono- and di-functionalized bistolane-based methacrylate monomers, substituted with one fluorine atom in the central rings, in order to synthesize uniaxial high-birefringence polymer films by means of a photo-crosslinking reaction.

Fig. 13. Molecular structure of bistolanes.

Chapter 4

In **Chapter 4**, the development of novel sulfur-containing calamitic LC materials is described. As mentioned in Section **4-4**, the development of these materials is very important for not only preparing high-birefringence materials, but also in terms of fundamental understanding of LC chemistry. Owing to strong intermolecular interactions, it is difficult to synthesize these materials with stable mesophases. Although I attempted to synthesize various calamitic molecules with alkylsulfanyl groups, all the molecules did not possess stable mesophases, as described in **Chapter 4-3**. Therefore, in order to realize calamitic LC molecules with alkylsulfanyl groups, I present the following two strategies - (1) introduction of fluorine at the central ring of bistolane-based molecules with alkylsulfanyl groups at both of the terminal positions and (2) using hydrogen bonding between carboxyl groups in tolane-based molecules. In the former case, since intermolecular interactions are decreased because of the presence of fluorine, it may lead to the presence of mesophases.[18] In the case of the latter, it is known that benzoic acid derivatives have mesophases,[42] since they can form structures with a great degree of anisotropy, owing to their dimerization. Furthermore, according to some reports in the literature, hydrogen bonding produces more molecular disorder than covalent bonding.[43] Therefore, I believe that hydrogen bonding can allow molecules to rotate and/or translate,

leading not only to expanded anisotropic structures, but also the formation of some mesophases.

On the other hand, in order to develop new thiophene-based calamitic molecules having nematic phases in a wide temperature range, I designed diaryl-diacetylene molecules with a thiophene-based, condensed, and di-cyclic structure. Diaryl-diacetylenes were selected as the core, since they tend to form nematic phases, owing to the slip alignments resulting from the dumbbell-like structure shown in **Chapter 1-2**. Moreover, in order to expand their anisotropic structures further, rings larger than the thiophenyl ring were introduced.

In **Chapter 4-1**, I describe the design of novel bistolane-based LC molecules fluorinated at the central rings. The phase transition behaviors of these molecules were investigated by POM observations and DSC measurements, and their birefringence properties were evaluated. Consequently, with the aim of developing materials with even wider nematic phases and higher birefringence properties, the design of methylthio group containing asymmetric bistolane-based molecules that have cyano or isothiocyanate groups at the other terminal positions is described in **Chapter 4-2**. In **Chapter 4-3**, I describe the design of a hydrogen-bonding tolane-based molecule with terminal carboxyl and alkylsulfanyl groups, in order to test a different strategy from those described in chapters **4-1** and **4-2**, for obtaining sulfur-containing calamitic LC molecules. In order to develop new high-birefringence thiophene-based nematic materials, the synthesis of four diaryl-diacetylene derivatives containing thiophenyl-benzene, benzothiophene, bithiophene, and thienothiophene as diaryl structures is described in **Chapter 4-4**, and their thermal transition behaviors and optical properties are investigated in detail.

General conclusion

With the goal of developing high-birefringence nematic LC materials, I have synthesized various π-conjugated calamitic (or rod-like) molecules based on diaryl-oligoyne and bistolane skeletons, and have evaluated their refractive indices and birefringence properties from single-component systems. In addition, I have analyzed the LC phase structures of these materials. The significance of this study lies in the fact that I have not only developed novel high-birefringence LC materials, but have also investigated the correlations between their optical properties, molecular polarizabilities, and assembly states. As described in Chapters 1 and 2, molecules with a large molecular polarizability anisotropy exhibited not only larger n_e, but also slightly larger n_o values, compared to molecules with smaller molecular polarizability anisotropy, resulting in larger birefringence. On the other hand, in the case of the polymers containing DNA moieties in the side chain (described in Chapter 2-4), the birefringence values were observed to increase with an increase in the molecular weight and were in the following order: monomer < oligomer < polymer. It may be noted that the birefringence values are different, even though the molecular polarizabilities of the three types of molecular units are comparable. In addition, even though sulfur-containing LC molecules exhibited larger molecular polarizabilities, these molecules exhibited not only larger n_e values, but also comparable or slightly smaller n_o values, resulting in higher birefringence compared to those of derivatives with alkoxy tails, as described in Chapters 4-1 and 4-2. These results are attributed to the fact that the order parameter (S) of the sulfur-containing LC molecules is increased as a result of polymerization and intermolecular attractive interactions of the sulfur atoms. In other words, the incorporation of conjugated structures in the side chain and the presence of sulfur-containing substitutions with specific attractive interactions are effective in improving the birefringence properties of these compounds. In the future, I hope that new nematic high-birefringence molecular designs and nematic LC polymer materials continue to

be developed for various practical applications.

Reference

1. (a) J. W. Goodby, P. J. Collings, T. Kato, C. Tschierske, H. Gleeson and P. Raynes, Handbook of liquid crystals, 8 Volume Set, 2nd Edition, Wiley-VCH, 2014; (b) J. W. Goodby, *Liq. Cryst.*, 2011, **38**, 1363; (c) P. Kirsch and M. Bremer., *Angew. Chem. Int. Ed.*, 2000, **39**, 4216; (d) R. Dąbrowski, P. Kula and J. Herman, *Crystals*, 2013, **3**, 443.
2. (a) M. Mitov, *Adv. Mater.*, 2012, **24**, 6260; (b) T. J. White, M. E. McConney and T. J. Bunning, *J. Mater. Chem.*, 2010, **20**, 9832. (c) D. J. Broer, J. Lub and G. N. Mol, *Nature*, 378, 467.
3. (a) H. Yu and T. Ikeda, *Adv. Mater.*, 2011, **23**, 2149; (b) A. Shishido, *Polym. J.*, 2010, **42**, 525;
4. H. R. Stapert, S. del Valle, E. J. K. Verstegen, B. M. I. ven der Zande, J. Lub and S. Stallinga, *Adv. Funct. Mater.*, 2003, **13**, 732.
5. T.-S. Chung, S.-X. Cheng, and M Jaffe, 2001. Liquid Crystalline Polymers, Main-Chain. Encyclopedia Of Polymer Science and Technology. 3.
6. F. C. Bawden and N. W. Pirie, *P. Roy. Soc. Lond. B Bio.*, 1937, **123**, 274
7. I. Dierking, Textures of Liquid Crystals, Wiley-VCH, 2003
8. M. F. Vuks, *Opt. Spektrosk.*, 1966, 20, 644.
9. M. J. Stephen and P. S. Joseph, "Physics of liquid crystals." Reviews of Modern Physics 1974, **46**, 617
10. (a) S.-T. Wu, *Phys. Rev. A*, 1986, **33**, 1270; (b) S.-T. Wu, *J. Appl. Phys.*, 1991, **69**, 2080; (c) J. Li and S.-T. Wu, *J. Appl. Phys.*, 2004, **95**, 896; (d) J. Li, *Student Member IEEE*, C.-H. Wen, S. Gauza, R. Lu, S.-T. Wu and *Fellow IEEE, J. Disp. Technol.*, 2005, 1, 51
11. G.W. Gray, K. J. Harrison and J. A. Nash, *Electronics Lett.*, 1973, **9**, 130.

12. (a) L. K. M. Chan, G. W. Gray and D. Lacey, *Mol. Cryst. Liq. Cryst.*, 1985, **123**, 185; (b) L. K. M. Chan, G. W. Gray and D. Lacey and K. J. Toyne, *Mol. Cryst. Liq. Cryst.*, 1988, **158B**, 209.
13. (a) S. Gauza, C.-H. Wen, S.-T. Wu, N. Janarthanan and C.-S. Hsu, *Jpn. J. Appl. Phys.*, 2004, **43**, 7634; (b) Y.-M. Liao, H.-L. Chen, C.-S. Hsu, S. Gauza and S.-T. Wu, *Liq. Cryst.*, 2007, **34**, 507; (c) X.-L. Guan, L.-Y. Zhang, Z.-L. Zhang, Z. Shen, X.-F. Chen, X.-H. Fan, Q.-F. Zhou, Tetrahedron, 2009, **65**, 3728; (d) A. J. Seed, K. Pantalone, U. M. Sharma and A. M. Grubb, *Liq. Cryst.*, 2009, **36**, 329.
14. (a) C. Sekine, N. Konya, M. Minai and K. Fujisawa, *Liq. Cryst.*, 2001, **28**, 1361; (b) C. Sekine, M. Ishitobi, K. Iwakura, M. Minai and K. Fujisawa, *Liq. Cryst.*, 2002, **29**, 355; (c) M. Hird, K. J. Toyne, J. W. Goodby, G. W. Gray, V. Minter, R. P. Tuffin and D. G. McDonnel, *J. Mater. Chem.*, 2004, **14**, 1731; (d) J. Herman, O. Chojnowska, P. Harmata, R. Dąbrowski, B. W. Klus and P. Kula, *Liq. Cryst.*, 2014, **41**, 1647.
15. (a) A. J. Seed, K. J. Toyne, J. W. Goodby and D. G. McDonnell, *J. Mater. Chem.*, 1995, **5**, 1; (b) A. J. Seed, K. J. Toyne, M. Hird and J. W. Goodby, *Liq. Cryst.*, 2012, **39**, 403.
16. (a) H. Takatsu, K. Takeuchi, Y. Tanaka, M. Sasaki, *Mol. Cryst. Liq. Cryst.*, 1986, 141, 279, (b) S.-T. Wu and C.-S. Hsu, *Proc. SPIE*, 1997, **3015**, 8 (c) G. W. Gray and S. M. Kelly, *J. Mater. Chem.*, 1999, **9**, 2037; M. D. Gupta, A. Mukhopadhyay, S. K. Roy and R. Dabrowski, *J. Appl. Phys.*, 2013, **113**, 053516.
17. (a) B. Grant, From Mol. Cryst. and Liq. Cryst., 1978, 48, 175; (b) S.-T. Wu, U. Finkenzeller and V. Reiffenrath, *J, Appl. Phys.*, 1989, 65, 4372; (c) S.-T. Wu, H.-H. B. Meng and L. R. Dalton, *J. Appl. Phys.*, 1991, **70**, 3013; (d) S.-T. Wu, J. D. Margerum, H. B. Meng, L. R. Dalton, C.-S. Hsu and S.-H. Lung, *Appl. Phys. Lett.*, 1992, **61**, 630 ; (e) S. T. Wu, J. D. Margerum, H. B. Meng, C. S. Hsu, and L. R. Dalton, *Appl. Phys. Lett.*, 1994, **64**, 1204; (g) Z.-C. Miao, D. Wang, Y.-M. Zhang, Z.-K Jin, F. Liu, F.-F Wang and H. Yang, *Liq. Cryst.*, 2012, **39**, 1291

18. M. Hird, *Chem. Soc. Rev.*, 2007, **36**, 2070.
19. A. De Vries, *Mol. Cryst. Liq. Cryst.*, 1970, **10**, 219.
20. (a) C. Tschierske and D. J. Photinos, *J. Mater. Chem.*, 2010, **20**, 4263; (b) E. T. Samulski, *Liq. Cryst.*, 2010, 37, 669.
21. C. Keith, A. Lehmann, U. Baumeister, M. Prehma and C. Tschierske, *Soft Matter*, 2010, **6**, 1704.
22. (a) P. Sarkar , P. K. Sarkar, S. Paul and P. Mandal, *Phase Transitions*, 2000, **71**, 1; (b) W. Nishiya, Y. Takanishi, J. Yamamoto and A. Yoshizawa, *J. Mater. Chem. C*, 2014, **2**, 3677.
23. K. Okano, A. Shishido and T. Ikeda, *Adv. Mater.*, 2006, **18**, 523–527.
24. K. Okano, O. Tsutsumi, A. Shishido, and T. Ikeda, *J. Am. Chem. Soc.*, 2006, **128**, 15368.
25. N. Kawatsuki, A. Yamashita, M. Kondo, T. Matsumoto, T. Shioda, A. Emoto and H. Ono, *Polymer*, 2010, **51**, 2849.
26. S. Chen, L.-Y. Zhang, X.-L. Guan, X.-H. Fan, Z. Shen, X.-F. Chen and Q.-F. Zhou, *Polym. Chem.*, 2010, **1**, 430.
27. J. Lub, D. J. Broer, M. E. M. Antonio and G. N. Mol, *Liq. Cryst.*, 1998, **24**, 375.
28. (a) A. J. Seed, K. J. Toyne, J. W. Goodby and M. Hird, *J. Mater. Chem.*, 2000, **10**, 2069; (b) A. J. Seed, K. Pantalone, U. M. Sharma and A. M. Grubb, *Liq. Cryst.*, 2009, **36**, 329.
29. (*a*) A. J. Seed, K. J. Toyne and J. W. Goodby, *J. Mater. Chem.*, 1995, **5**, 2201; (*b*) G. J. Cross, A. J. Seed, K. J. Toyne, J. W. Goodby, M. Hird and M. C. Artal, *J. Mater. Chem.*, 2000, **10**, 1555.
30. (a) T. M. Barclay, A. W. Cordes, R. C. Haddon, M. E. Itkis, R. T. Oakley, R. W. Reed and H. Zhang, *J. Am. Chem. Soc.*, 1999, **121**, 969; (b) K. Kobayashi, H. Masu, A. Shuto and K. Yamaguchi, *Chem. Mater.*, 2005, **17**, 6666.
31. (a) Y. Mazaki and K. Kobayashi, *J. Chem. Soc. Perkin Trans. 2*, 1992, 761; (b) J. Dai, M. Munakata, L.-P. Wu, T. Kuroda-Sowa and Y. Suenaga, *Inorg. Chim. Acta*, 1997,

258, 65; (c) M. Iwaoka, S. Takemoto, M. Okada and S. Tomoda, *Bull. Chem. Soc. Jpn.*, 2002, **75**, 1611; (d) D. B. Werz, R. Gleiter and F. Rominger, *J. Am. Chem. Soc.*, 2002, **124**, 10638.

32. (a) D. Miyajima, F. Araoka, H. Takezoe, J Kim, K. Kato, M. Takata, T. Aida, *Science*, 2012, **336**, 209; (b) D. Adam, P. Schumacher, J. Simmerer, L. Haussling, K. Siemensmeyer, K. H. Etzbach, H. Ringsdorf and D. Haarer, *Nature*, 1994, **371**, 141; (c) F. Nekelson, H. Monobe, M. Shiro and Y. Shimizu, *J. Mater. Chem*., 2007, **17**, 2607; (d) S. Kumar, *Liq Cryst*., 2004, **31**, 1037.

33. (a) I. C. Pintre, J. L. Serrano, M. B. Ros, J. Ortega, I. Alonso, J. M. Perdiguero, C. L. Folcia, J. Etxebarria, F. Goc, D. B. Amabilino, J. P. Luis and E. G. Nadal, *Chem. Commun.*, 2008, 2523; (b) S. Kang, M. Harada, X. Li, M. Tokita and J. Watanabe, *Soft Matter*, 2012, **8**, 1916; (c) G. Heppke, D. D. Parghi and H. Sawade, *Liq Cryst*., 2000, **27**, 313.

34. (a) M. Funahashi and J. Hanna, *Adv. Mater*., 2005, **17**, 594; (b) T. Yasuda, T. Shimizu, F. Liu, G. Ungar and T. Kato, *J. Am. Chem. Soc*., 2011, **133**, 13437; (c) D. Miyajima, F. Araoka, H. Takezoe, J. Kim, K. Kato, M. Takata and Y. Aida, *Angew. Chem. Int. Ed*., 2011, **50**, 7865.

35. (a) A. J. Seed, K. J. Toyne and J. W. Goodby, *J. Mater. Chem*., 1995, **5**, 653; (b) N. L. Campbell, W. L. Duffy, G. I. Thomas, J. H. Wild, S. M. Kelly, K. Bartle, M. O'Neill, V. Minter, R. P. Tuffin, *J. Mater. Chem*., 2002, **12**, 2706.

36. (a) R. Brettle, D. A. Dunmur, C. M. Marson, M. Pinol and K. Toriyama, *Chem. Lett*., 1992, 613; (b) R. Brettle, D. A. Dunmur, C. M. Marson, M. Pinol and Toriyama K. *Liq. Cryst*., 1993, **13**, 515; (c) S. Kuiper, W. F. Jager, T. J. Dingemans and S. J. Picken, *Liq. Cryst*., 2009, **36**, 389.

37. (a) Y. Rubin, S. S. Lin, C. B. Knobler, J. Anthony, A. M. Boldi and F. Diederich, *J. Am. Chem. Soc.*, 1991, **113**, 6943; (b) R. R. Tykwinski, T. Luu, *Synthesis*, 2012, **44**, 1915; (c) G. Chen, I. Mahmud, L. N. Dawe, L. M. Daniels and Yuming Zhao, *J. Org. Chem.*, 2011, **76**, 2701; (d) F. Ye, A. Orita, J. Yaruva, T. Hamada and J. Otera, *Chem. Lett*. 2004, **33**, 528.

38. M. Uchimura, S. Kang, R. Ishige, J. Watanabe and G. Konishi, *Chem. Lett.*, 2010, **39**, 513.

39. H.-F. Hsu, Y.-H. Lai, S.-Y. Lin, W.-C. Lin and J.-F. Chen, *Liq. Cryst.*, 2003, **30**, 325.

40. C. Pugh and V. Percec, *Polym. Bull.*, 1990, **23**, 177.

41. (a) S.-T. Wu, C.-S. Hsu, Y.-Y. Chuang, *Jpn, J, Appl, Phys.*, 1999, **38**, L286; (b) S.-T. Wu, C.-S. Hsu, Y.-Y. Chuang and H.-B. Cheng, *Jpn, J, Appl, Phys.*, 2000, **39**, L38; (c) Y.-M. Zhang, D. Wang, Z.-C. Miao, S.-K Jin and H. Yang, *Liq. Cryst.*, 2012, **39**, 1330.

42. (a) A. E. Bradfield and B. Jones, *J. Chem. Soc.*, 1929, 2660; (b) G. W. Gray and B. Jones, *J. Chem. Soc.*, 1953, 4179; (c) A. J. Herbert, *Trans. Faraday Soc.*, 1967, **63**, 555; (d) C. Kavitha, N. P. S. Prabu, M. L. N. M. Mohan, *Mol. Cryst. Liq. Cryst*., 2014, **592**, 163; (e) M. Roohnikan, M. Ebrahimi, S. R. Ghaffarian and N. Tamaoki, *Liq. Cryst*., 2013, **40**, 314

43. (a) E. Barmatov, S. Grande, A. Filippov, M. Barmatova, F. Kremer and V. Shibaev, *Macromol. Chem. Phys*., 2000, **201**, 2603; (b) Y. Uchida, K. Suzuki and R. Tamura, *J. Phys. Chem. B*, 2012, **116**, 9791; (c) W. He, G. Pan, Z. Yang, D. Zhao, G. Niu, W. Huang, X. Yuan, J. Guo, H. Cao and H. Yang, *Adv. Mater*., 2009, **21**, 2050.